

# Computer Simulation of the Photoluminescence of Nanostructured Aluminum Oxide Excited with Pulsed Synchrotron Radiation

V. S. Kortov, T. V. Spiridonova, and S. V. Zvonarev

*Institute of Physics and Technology, El'tsyn Ural Federal University, Yekaterinburg, 620002 Russia*

*e-mail: VSKortov@mail.ru, forSpiridonova@gmail.com, s.v.zvonarev@ustu.ru*

Received January 25, 2013

**Abstract**—An algorithm and a program are developed to calculate the photoluminescence (PL) parameters for bulk single-crystal and nanoscale dielectrics excited with pulsed synchrotron radiation. The luminescence spectra of  $F$  and  $F^+$  centers and the PL decay kinetics in single-crystal and nanoscale aluminum-oxide samples containing oxygen anion vacancies are calculated for various nanoparticle sizes. It is shown that a noticeable broadening of the bands and a decrease in the afterglow time is observed for nanoparticle sizes that are less than 20 nm.

**DOI:** 10.1134/S1027451013050327

## INTRODUCTION

Aluminum oxide is a multifunctional material, which is widely used in science and technology. Its structural defects and optical and luminescence properties are studied intensively. Highly sensitive detectors of ionizing radiation [1, 2] are fabricated using  $\alpha$ - $\text{Al}_2\text{O}_3$  crystals containing anion vacancies, and nanostructured corundum is regarded as a promising material for high-dose measurements [3].

It is well known that many properties of corundum under study are determined by the concentration of  $F$  centers (oxygen vacancies with two captured electrons) and  $F^+$  centers (oxygen vacancies with one captured electron) [4]. The maximum of the optical absorption band for  $F$  centers is located at 6.1 eV, which causes difficulties upon the excitation of these centers with ultraviolet radiation in the atmosphere. In addition, corundum is a wide-gap dielectric ( $E_g = 9.4$  eV). Therefore, its photoluminescence properties can be effectively studied under excitation in regions of the fundamental-absorption tail and intracenter transitions in  $F^-$  and  $F^+$  centers only in the case of photon energies of 10 eV or more.

It is worthwhile studying the PL properties in the indicated range using synchrotron radiation (SR). A series of papers [4, 5] is dedicated to studying corundum containing anion vacancies with the use of SR for its excitation (including time-resolved studies). The authors of these papers obtained new results on the excitation transport and the specificity of intracenter transitions and presented proof of the existence of excitons related to defects and of their participation in PL processes [6, 7]. Single crystal and nanoscale samples were studied in these cases. As a result, it was

proved that using SR to study the luminescence properties of corundum in its various structural states is very effective and informative. However, studies using SR remain expensive, while studying the properties of nanoscale dielectrics for the purpose of producing new functional materials is being broadened continuously. It is necessary to note that the fabrication and certification of nanoscale samples are difficult problems requiring the use of expensive equipment. In connection with this, computer simulation of the spectral-kinetic PL properties of nanostructured materials excited with SR photons makes it possible to considerably cut down expenses and time spent on seeking for new functional materials and on producing them.

The aim of this paper is the development of a physical model and computer simulation of the luminescence spectra and the PL decay kinetics under the excitation of single-crystal and nanostructured  $\alpha$ - $\text{Al}_2\text{O}_3$  samples containing anion vacancies with pulsed SR.

## DESCRIPTION OF THE MODEL

The interaction processes of pulsed SR with a dielectric and the subsequent PL are considered in our model. The physical model and the mathematical description of the PL processes were developed for a dielectric material, in particular, for  $\alpha$ - $\text{Al}_2\text{O}_3$ , which was excited with a pulse of photons with an energy of 10 eV and a duration of 1 ns. The PL-excitation parameters corresponded to the characteristics of the DESY synchrotron (Hamburg) [8], which provides the opportunity to compare the calculated results with the experimental data obtained using this synchrotron source.

In the first approximation, the process of PL excitation with photons with energies exceeding the width of the band gap of the dielectric can be represented as follows. Upon excitation of the dielectric, photons transfer their energies to electrons which leave the atom and transit to the conduction band. Fast photoelectrons produced by quanta experience inelastic scattering at valence electrons with the creation of secondary nonequilibrium electron–hole pairs [9]. The position of the boundary of the onset of the process of electron–hole pair generation is related to the ratio of the effective electron and hole masses. Next, electrons and holes can recombine with a transfer of their energy to luminescence centers and with subsequent luminescence of the excited state of the center in the corresponding spectral band.

The physical model used to calculate the luminescence parameters under pulsed excitation with SR photons contains the following main events:

1. *Generation of electron–hole pairs and the establishment of their quasi-equilibrium concentration at the instant of SR pulse termination.* The generation rate is calculated using formula [10]:

$$G = 6.25 \times 10^{15} P_\gamma \rho / E_i, \quad (1)$$

where  $P_\gamma$  is the power of the ionizing radiation dose,  $\rho$  is the density of the irradiated material, and  $E_i$  is the energy of electron–hole pair formation calculated in accordance with [11].

The main energy of the absorbed photon energy is ionizing. The radiation-dose power  $P_\gamma$  can be determined as follows: [10]

$$P_\gamma = 1.6 \times 10^{-10} E_{\text{exc}} \phi_\gamma \mu / \rho, \quad (2)$$

where  $E_{\text{exc}}$  is the energy of photons exciting PL,  $\mu$  is the linear coefficient of photon-energy absorption, and  $\phi_\gamma$  is the density of the SR radiation quantum flux.

The formula used to determine the linear absorption coefficient has the form [12]

$$\mu(E) = \mu_m \exp\left[(-4 \ln 2 / \Delta^2)(E_m - E_{\text{exc}})^2\right], \quad (3)$$

where  $\mu_m$  is the maximum absorption coefficient (it has different values for each band),  $\Delta$  is the width of the PL band (if the peak has Gaussian form, then the band width is determined at a level of 0.63 of the maximum intensity), and  $E_m$  is the energy position of the luminescence-band maximum.

The variation in the concentration  $n_{\text{eh}}$  of the electron–hole pairs is calculated using the kinetic balance equation [13]:

$$dn_{\text{eh}}/dt = G - An_{\text{eh}} - Bn_{\text{eh}}^2, \quad (4)$$

where  $A$  and  $B$  are the total coefficients of linear and quadratic recombination of electron–hole pairs at luminescence centers. During the action of a photon

pulse of rectangular form, the solution of Eq. 4 for the initial condition  $t = 0, n_{\text{eh}} = 0$  has the form [14]

$$n_{\text{eh}} = 2G\tau_i \left( e^{t/\tau_i} - 1 \right) / \left( \delta e^{t/\tau_i} + \gamma \right), \quad (5)$$

$$\tau_i = 1 / \left( 4BG + A^2 \right)^{1/2}.$$

Here,  $\tau_i$  is the characteristic ionization time and  $\delta$  and  $\gamma$  are variables, which are dependent on the coefficient of linear recombination and on the characteristic ionization time. After the action of the photon pulse ( $t > t_p, G = 0$ ) (irrespective of its shape) is terminated, the expression for the concentration of electron–hole pairs becomes [14]:

$$n_{\text{eh}} = A\alpha / [B(\exp[A(t - t_p)] - \alpha)], \quad (6)$$

$$\alpha = Bn_{\text{eh}0} / (A + Bn_{\text{eh}0}),$$

where  $t_p$  is the duration of the photon-beam pulse and  $n_{\text{eh}0}$  is the concentration of electron–hole pairs at the pulse end and is determined by expression (5) for  $t = t_p$ .

2. *Recombination of charge carriers with the excitation of intracenter transitions and formation of the luminescence band.* In the corundum crystals under study, the luminescence of  $F$  and  $F^+$  centers is realized in accordance with the intracenter PL mechanism [15]. Intracenter PL is produced because of optical transitions between local levels of the luminescence center. Recombination with the participation of local levels can be implemented in the form of the capture of electron–hole pairs by luminescence centers. The total coefficients  $A$  and  $B$  of electron–hole pair recombination at luminescence centers can be calculated as follows [14]:

$$A = \sigma v_e N_c, \quad (7)$$

$$B = \sigma v_e 4/3 \pi l^3 N_c, \quad (8)$$

where  $\sigma$  is the effective transverse cross section for the capture of free electrons (holes) by luminescence centers, whose concentration is  $N_c$ ;  $v_e$  is the velocity of free charge carriers; and  $l$  is the mean free path of the electron (hole).

The luminescence band forms during the action of the photon pulse when recombination processes and intracenter transitions occur. Experiments show that it has Gaussian form. In our paper, taking the indicated physical processes into account, we propose the following relation to describe bands in the PL spectra  $I(h\nu)$ :

$$I(h\nu) = \left[ 1 / \left( U (\pi/2)^{1/2} \right) \right] \times \int_0^d G \exp\left( -(2[E_{\text{exc}} - E_m]/U)^2 \right) dx, \quad (9)$$

where  $U$  is the luminescence line half-width,  $G$  is the rate of electron–hole generation,  $E_m$  is the energy peak position, and  $d$  is the sample thickness.

It is well known that the luminescence bands broaden in nanostructured materials. The spectral-band width is due to the action of two factors: electron scattering at crystal-lattice defects and electron–phonon interaction. The processes of electron scattering make the main contribution, which depends on the surface fraction and is proportional to  $\sim 1/R$ . The contribution of the electron–phonon interaction corresponds to  $\sim 1/R^2$  [16]. Thus, the change in the line width  $\Delta U$  can be described by the formula:

$$\Delta U = h v_F / R + \varphi(R) / R^2, \quad (10)$$

where  $v_F$  is the electron velocity on the Fermi surface,  $h$  is Planck's constant,  $\varphi(R)$  is the function dependent on the particle size, and  $R$  is the particle size.

3. *Decay of intracenter PL.* The time variation in the intracenter PL intensity  $I_c$ , i.e., the decay kinetics, is determined by the occupation  $N_i$  of the radiation level and by the probability  $A_{i0}$  of optical transition from this level to the ground state [13]:

$$I_c(t) = E_m A_{i0} N_i(t), \quad (11)$$

where  $E_m$  is the photon energy (the maximum position in the emission spectrum). The kinetic equation for occupation of the  $i$ th radiation level of the luminescence center in the irradiated material area has the form [14]:

$$\frac{dN_i}{dt} = B_{ief} n_{eh}^2 - (A_{i0} + A_{ip}) N_i, \quad (12)$$

where  $A_{ip}$  is the probability of a nonradiative transition and  $B_{ief}$  is the effective constant of the excitation rate of the radiation level.

The kinetics of the PL intensity variation can be described as follows [14]:

$$I_c(t) = I_c(t_p) \left( f(z) + e^{-A_i(t-t_p)} \right), \quad t_p \leq t \leq t_1, \quad (13)$$

$$\begin{aligned} I_c(t) &= I_c(t_1) \\ &\times \left[ A^2 \left( e^{-A_i(t-t_1)} - e^{-2A_i(t-t_1)} \right) / A_i (2A - A_i) + e^{-A_i(t-t_1)} \right], \quad (14) \\ &t > t_1, \end{aligned}$$

where  $z = z_0 + A_i(t - t_p)$ ;  $z_0 = A_i \tau_{rec}$ ;  $f(z)$  is the function described in [14]; and  $I_c(t_p)$  and  $I_c(t_1)$  are the intensities at the instant of photon-pulse termination and at the instant  $t_1$ , respectively. The time instant  $t_1$  divides the time dependence of the luminescence intensity into qualitatively distinguished time intervals: near ( $t_p \leq t \leq t_1$ ) and far ( $t > t_1$ ) afterglow. The quantity  $t_1$  can be defined as [14]:

$$t_1 \approx t_p + 1/A. \quad (15)$$

When describing the PL decay kinetics in nanostructured dielectrics, it is necessary to additionally take

into account the variation in the excitation relaxation time  $\tau$ , which is described by the formula [16]

$$1/\tau = a R^\alpha / \tau_b + b v_e / R, \quad (16)$$

where  $a$  and  $b$  are constants,  $\tau_b$  is the relaxation time in a solid material,  $v_e$  is the kinetic velocity of free charge carriers, and  $R$  is the particle size.

## SIMULATION RESULTS AND DISCUSSION

Based on the described physical model, we developed an algorithm for calculating the luminescence spectra and the decay kinetics in dielectric materials under pulsed excitation with a photon beam. Based on the obtained algorithm, we developed a program in the Object Pascal program language in the Delphi 7 medium.

As was mentioned above,  $F$  and  $F^+$  centers (the most studied types of defects in this material, although their structures and spectral properties cannot be regarded as fully established) are the main centers in the  $\alpha$ - $\text{Al}_2\text{O}_3$  crystals under study containing anion vacancies. Excitation of an  $F$  center with ultra-violet radiation in the absorption band at 6.1 eV produces luminescence with a band maximum at 3.0 eV (410 nm) (singlet–triplet transition) [15]. The excited state of the  $F^+$  center is split into three states, which can be explained by the influence of the crystal field because of the low crystal symmetry. The absorption bands at 4.8, 5.4, and 6.3 eV correspond to transitions from the ground to the excited states. Luminescence at 3.8 eV (320 nm) occurs in the case of the excitation of  $F^+$  center with photons in the indicated absorption bands [17].

In the  $\alpha$ - $\text{Al}_2\text{O}_3$  crystal under study containing anion vacancies, centers producing luminescence are transformed as follows: for an  $F$  center,  $\bar{e} + F^+ \rightarrow F^* \rightarrow F$  (3.0 eV), and, for an  $F^+$  center,  $h^+ + F \rightarrow F^{+*} \rightarrow F^+$  (3.8 eV) [15].

The PL spectra for the  $\alpha$ - $\text{Al}_2\text{O}_3$  crystal were calculated for the following parameters: the SR pulse duration  $t = 1$  ns, the energy of exciting photons  $E_{exc} = 10$  eV ( $\lambda_{exc} = 123.65$  nm), the sample temperature  $T = 300$  K, and the thickness of the luminescent layer of the  $\alpha$ - $\text{Al}_2\text{O}_3$  sample is  $d = 100$  nm. The luminescent-layer thickness was chosen by taking into account the sample transparency and the penetration depth of the exciting SR quanta with the chosen energy (i.e., with  $\lambda_{exc}$ ). The nanostructured  $\alpha$ - $\text{Al}_2\text{O}_3$  samples are nontransparent, a thin porous surface layer with a thickness of no more than 100 nm luminesces in them [18]. Based on experimental data, the function  $\varphi(R)$  was assumed to be unity. In our calculations, we also used the following constants: the width of the band gap

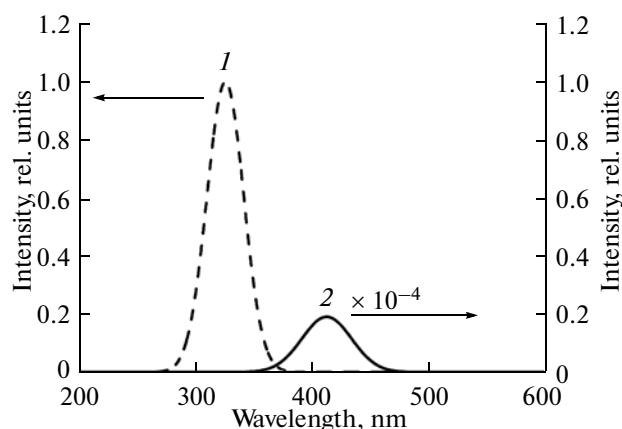


**Fig. 1.** PL spectra of (1)  $F^+$  and (2)  $F$  centers in a single-crystal  $\alpha\text{-Al}_2\text{O}_3$  sample under excitation with a pulsed photon beam ( $E_{\text{exc}} = 10$  eV).

$E_g = 9.4$  eV, the concentration of  $F$  centers  $N_F = 10^{17} \text{ cm}^{-3}$ , the concentration of  $F^+$  centers  $N_{F^+} = 10^{18} \text{ cm}^{-3}$  [6], and the probabilities of optical transitions at the  $F$  and  $F^+$  centers were chosen as  $A_F = 0.3 \times 10^{10} \text{ s}^{-1}$  and  $A_{F^+} = 1.5 \times 10^2 \text{ s}^{-1}$ , respectively.

To verify the adequacy of the developed physical model, we calculated the PL spectra of a  $\alpha\text{-Al}_2\text{O}_3$  single-crystal sample containing anion vacancies (Fig. 1). For excitation with a nanosecond photon pulse, the band intensity of the  $F^+$  center is dominant over that of the  $F$  center. The luminescence band of the  $F$  center has a maximum at 412 nm. The PL maximum of the  $F^+$  center is located in the range of smaller wavelengths (325 nm) with respect to the luminescence peak of the

$F$  center. The obtained luminescence-band parameters correspond to the indicated published data [15].

For the chosen parameters, we also calculated the PL spectra of the  $F$  and  $F^+$  centers in the nanostructured  $\alpha\text{-Al}_2\text{O}_3$  sample with different particle sizes and compare them with those in the single-crystal sample (Figs. 2 and 3).

It can be seen that, as the particle size decreases, the PL intensity decreases and the half-width of the luminescence line increases, which is due to the processes of electron scattering at defects of the crystal lattice and of electron–phonon interaction. The processes of electron scattering at defects concentrated on nanoparticle surfaces make the largest contribution to PL-band broadening. As follows from the data in Fig. 3, a significant change in the half-width of the PL band is observed for nanoparticle sizes of 20 nm or less.

Simulation of the PL decay kinetics in the single-crystal  $\alpha\text{-Al}_2\text{O}_3$  containing anion vacancies showed that the luminescence of  $F^+$  centers with the decay time  $\tau_{F^+} = 1.5$  ns is dominant in the nanosecond relaxation time range, and the luminescence of  $F$  centers with the decay time  $\tau_F = 35$  ns is dominant in the millisecond one. A typical curve for  $F$ -center PL decay is shown in Fig. 4. The obtained results agree well with the data in [15], where the indicated parameters are  $\tau_{F^+} = 2.1$  and  $\tau_F = 34$  ms, respectively. The close values of the calculated and experimental data characterizing the PL decay kinetics in  $\alpha\text{-Al}_2\text{O}_3$  demonstrate the adequacy of the physical model once again.

To compare the peculiarities of the PL processes in nanostructured and single-crystal  $\alpha\text{-Al}_2\text{O}_3$ , we calculated the PL decay kinetics of  $F$  centers in the nano-

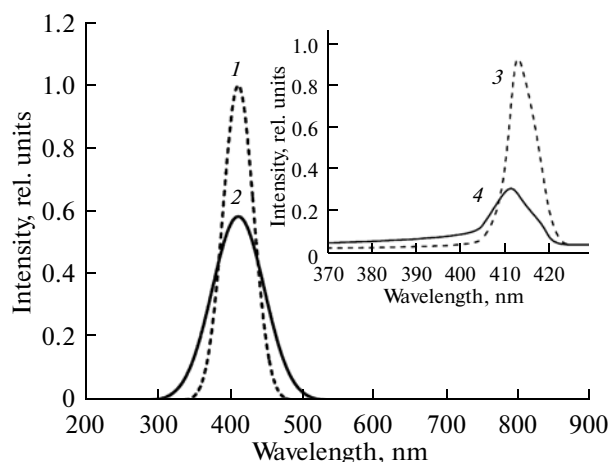


**Fig. 2.** Calculated PL spectra of  $F$  centers in (1) single-crystal and (2) nanostructured  $\alpha\text{-Al}_2\text{O}_3$  samples with particle sizes of 10 nm. They are compared with the experimental data for (3) single-crystal and (4) nanostructured  $\alpha\text{-Al}_2\text{O}_3$  samples [18].

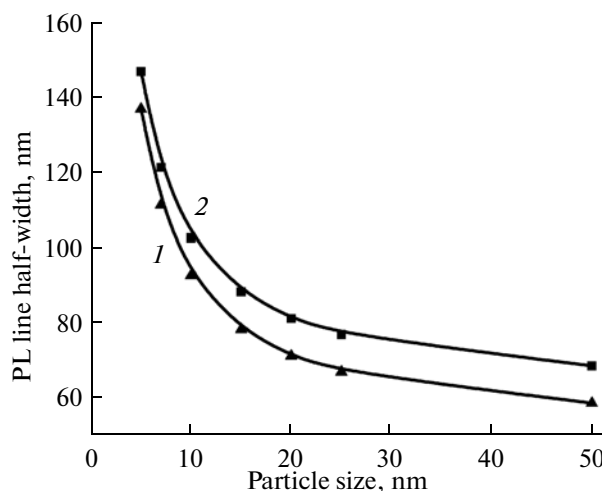


**Fig. 3.** Dependence of the PL line half-width of (1)  $F^+$  and (2)  $F$  centers on the particle size of nanostructured  $\alpha\text{-Al}_2\text{O}_3$  under excitation with SR.

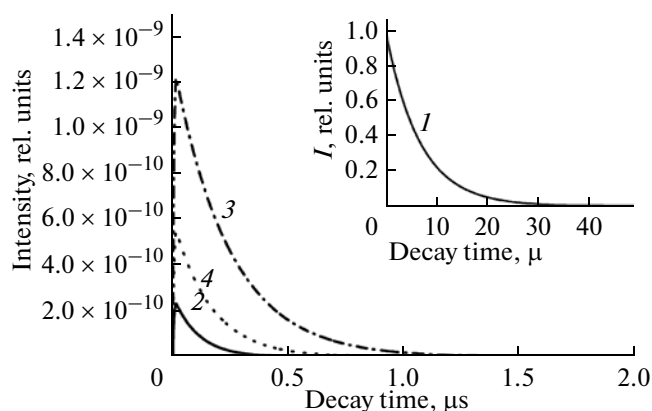


**Fig. 4.** PL decay kinetics for  $F$  centers after irradiation with a pulsed photon beam in (1) single-crystal and nanostructured  $\alpha$ - $\text{Al}_2\text{O}_3$  samples with particle sizes of (2) 50, (3) 20, and (4) 10 nm.

structured  $\alpha$ - $\text{Al}_2\text{O}_3$  samples with particle sizes of 5, 10, 20, and 50 nm for the indicated excitation parameters. The results are given in Fig. 4 and in the table, where the obtained values of the time  $\tau_e$  corresponding to the decrease in the PL intensity by a factor of  $e$  are shown. It follows from analysis of the data given in the table that, in nanostructured  $\text{Al}_2\text{O}_3$ , the decrease in the particle size first leads to an increase in the PL decay time; the latter requires a shorter time, as the particle sizes continue to decrease. The increase in the decay time is due to an increase in the relaxation time because of a decrease in electron–phonon interaction. Further, because of the increase in electron scattering at nanoparticle surfaces, the rate of electron relaxation increases and the PL decay time decreases as the nanoparticle sizes decrease [16].

PL decay of an  $F$  center in  $\alpha$ - $\text{Al}_2\text{O}_3$

Quantity $\tau_e$				
Single crystal	Nanoscale samples with different particle sizes			
	50 nm	20 nm	10 nm	5 nm
6.7 ms	0.12 $\mu\text{s}$	0.25 $\mu\text{s}$	0.17 $\mu\text{s}$	0.09 $\mu\text{s}$

It was established that the PL decay time of the  $F$  centers decreases to fractions of a microsecond as the particle sizes in nanostructured  $\alpha$ - $\text{Al}_2\text{O}_3$  decrease. The obtained data agree with the data in [18], where it was shown that  $\tau_F$  is 0.74  $\mu\text{s}$  for the  $\alpha$ - $\text{Al}_2\text{O}_3$  sample with an average particle size of 60 nm and is 0.25  $\mu\text{s}$  for the sample with an average particle size of 15 nm. Based on the experimental data and taking into account regularities of the physical processes, we can suggest that the PL decay of  $F^+$  centers in nanostructured  $\alpha$ - $\text{Al}_2\text{O}_3$  occurs in the picosecond range as the nanoparticle sizes decrease.

## CONCLUSIONS

Using the developed physical model and program complex, we have simulated PL decay kinetics and have calculated the luminescence spectra of single-crystal and nanostructured  $\alpha$ - $\text{Al}_2\text{O}_3$  samples containing anion vacancies under excitation with SR pulses with photon energies of 10 eV. The calculated band maxima of  $F$  and  $F^+$  centers in the PL spectra of the samples under study were close to the experimental data. Luminescence-band broadening dependent on particle sizes was observed for nanostructured aluminum oxide.

As the particle sizes decrease, the PL decay kinetics of  $F$  centers in the single-crystal and nanostructured  $\alpha$ - $\text{Al}_2\text{O}_3$  samples under SR pulsed excitation are significantly different. For the nanostructured samples, the afterglow time decreases by one order or more. In this case, the dependence of the PL decay time on the nanoparticle size is nonmonotonic: the afterglow duration increases as the nanoparticle sizes range from 50 to 20 nm and decreases as the nanoparticle sizes continue to decrease. Good agreement between the calculated and experimental data was obtained.

## REFERENCES

1. M. S. Akselrod, V. S. Kortov, D. J. Kravetsky, et al., *Radiat. Prot. Dosim.* **32**, 15 (1990).
2. V. S. Kortov, *Radiat. Meas.* **45**, 512 (2010).
3. N. Salah, Z. Khan, and S. Habib, *Nucl. Instrum. Methods Phys. Res. B* **269**, 401 (2011).
4. M. Kirm, E. Feldbach, A. Kotlov, et al., *Radiat. Meas.* **45**, 618 (2010).
5. S. V. Gorbunov, A. F. Zatsepin, V. A. Pustovarov, et al., *Phys. Solid State* **47**, 733 (2005).
6. A. I. Surdo, *Radia. Meas.* **42**, 763 (2007).
7. V. Yu. Ivanov, V. A. Pustovarov, and A. V. Kruzhalov, *J. Surf. Invest.: X-ray, Synchrotron Neutron Tech.* **4**, 671 (2010).
8. G. Zimmerer, *Radiat. Meas.* **42**, 859 (2007).
9. I. M. Ternov, V. V. Mikhailin, and V. R. Khalilov, *Synchrotron Radiation and its Application* (Mosk. Gos.

- Univ., Moscow, 1985; Harwood Academic, Amsterdam, 1985).
10. V. T. Gromov, *Introduction to Radiation Physics of Solids* (RFYaTs - VNIITF, Snezhinsk, 2007) [in Russian].
  11. R. C. Alig and S. Bloom, Phys. Rev. Lett. **35**, 1522 (1975).
  12. C. F. Yen and R. L. Coble, J. Am. Ceram. Soc. **62**, 89 (1979).
  13. V. V. Antonov-Romanovskii, *Photoluminescence Kinetics of Crystalline Phosphors* (Nauka, Moscow, 1966) [in Russian].
  14. V. I. Solomonov, Opt. Spectrosc. **95**, 248 (2003).
  15. A. I. Surdo, V. A. Pustovarov, V. S. Kortov, et al., Nucl. Instrum. Methods Phys. Res. A **543**, 234 (2005).
  16. I. P. Suzdalev, *Nanotechnology: Physicochemistry of Clusters, Nanostructures and Nanomaterials* (KomKniga, Moscow, 2006) [in Russian].
  17. B. D. Evans, J. Nucl. Mater. **219**, 202 (1995).
  18. V. S. Kortov, A. E. Ermakov, A. F. Zatsepin, et al., Phys. Solid State **50**, 957 (2008).

*Translated by L. Kul'man*